

State-to-state and simplified models for shock heated reacting air flows

O. Kunova, E. Nagnibeda, and I. Sharafutdinov

Citation: [AIP Conference Proceedings](#) **1628**, 1194 (2014); doi: 10.1063/1.4902728

View online: <http://dx.doi.org/10.1063/1.4902728>

View Table of Contents: <http://scitation.aip.org/content/aip/proceeding/aipcp/1628?ver=pdfcov>

Published by the [AIP Publishing](#)

Articles you may be interested in

[The influence of state-to-state kinetics on diffusion and heat transfer behind shock waves](#)

AIP Conf. Proc. **1628**, 1202 (2014); 10.1063/1.4902729

[Reacting gas mixtures in the state-to-state approach: The chemical reaction rates](#)

AIP Conf. Proc. **1628**, 1186 (2014); 10.1063/1.4902727

[State-to-State Kinetic Theory Approach for Transport and Relaxation Processes in Viscous Reacting Gas Flows](#)

AIP Conf. Proc. **1333**, 1371 (2011); 10.1063/1.3562834

[Modelling of arc jet plasma flow in transitional regime by Navier Stokes and state-to-state coupling](#)

AIP Conf. Proc. **762**, 1125 (2005); 10.1063/1.1941685

[State-to-state Kinetics and Transport Properties of a Reactive Air Flow Near a Re-entering Body Surface](#)

AIP Conf. Proc. **762**, 1061 (2005); 10.1063/1.1941675

State-to-State and Simplified Models for Shock Heated Reacting Air Flows

O. Kunova, E. Nagnibeda and I. Sharafutdinov

Saint Petersburg State University, 198504, Universitetskiy pr., 28, Saint Petersburg, Russia

Abstract. Hypersonic flows of the five-component air mixture $N_2/O_2/NO/N/O$ in the relaxation zone behind shock waves are studied on the basis of the state-to-state, three-temperature and one-temperature kinetic theory approaches. The equations of non-equilibrium vibrational and chemical kinetics are coupled to the gas dynamic equations and solved numerically for Mach numbers in the free stream $M = 15$. The results obtained using different approaches are compared and the influence of the kinetic model on the vibrational distributions, gas temperature, velocity and mixture composition is shown.

Keywords: non-equilibrium kinetics, exchange reactions, vibrational distributions

PACS: 47.70.Fw, 82.20.-w, 82.40.Fp

INTRODUCTION

Modeling of non-equilibrium kinetics in shock heated air flows is important for prediction of flow parameters near different bodies moving with high velocities in the Earth atmosphere, in experiments in shock tubes, for combustion processes and other applications. The detailed description of non-equilibrium reacting flows is based on coupling of state-to-state vibrational-chemical kinetics to gas dynamics [1]. This approach received much attention in the last decade for study of different flows of air components but mainly for binary mixtures of molecules and atoms N_2/N and O_2/O . The detailed state-to-state model of the five-component air mixture was applied for the nozzle flows in Ref. [2, 3], for the boundary layer near re-entering bodies in Ref.[4], for the flows in shock tubes [5].

Numerical simulations of multi-component reacting flows with the use of the state-to-state kinetic model are rather computationally consuming because of a large number of equations for vibrational level populations for each chemical species. Therefore the reduced description of vibrational-chemical kinetics in multi-component reacting mixtures [6, 7] is of interest for practical applications, particularly if many test-cases should be calculated.

In the present paper, the flows of air mixture $N_2(i)/O_2(i)/NO/N/O$ behind shock waves are studied within the detailed state-to-state approach and two reduced kinetic models based on the two-temperature and one-temperature vibrational distributions. The accuracy of reduced models is estimated comparing the results obtained in the state-to-state and simplified approximations. In calculations, the accurate anharmonic oscillator model for vibrational spectra of air components is used as well as vibrational energy expressions for harmonic oscillators and estimations of anharmonic effects on shock heated flow parameters are presented.

KINETIC SCHEME. GOVERNING EQUATIONS IN THE STATE-TO-STATE APPROACH

The full kinetic scheme for the considered mixture includes:

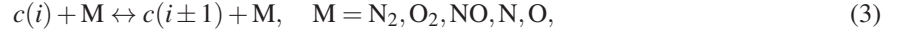
- VV vibrational energy exchanges at the collisions of molecules of the same species

$$c(i) + c(k) \leftrightarrow c(i \pm 1) + c(k \mp 1), \quad c = N_2, O_2, \quad (1)$$

- VV' exchanges between the molecules of various species

$$c(i) + d(k) \leftrightarrow c(i \pm 1) + d(k \mp 1), \quad d = N_2, O_2, \quad d \neq c, \quad (2)$$

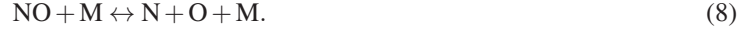
- VT (TV) exchanges between vibrational and translational energies



- two Zeldovich exchange reactions of NO formation



- dissociation and recombination



Here i and k are the vibrational states of colliding molecules.

Following [8, 9, 10, 11] we do not take into account vibrational excitation of NO molecules formed in result of reactions (4)-(5) and assume that they remain in the ground vibrational state during relaxation processes. In the state-to-state approach the non-equilibrium flow of considered mixture is described by the equations for vibrational level populations n_{N_2i} , n_{O_2i} , number densities of nitrogen oxide molecules n_{NO} and atoms n_N , n_O , macroscopic velocity v and gas temperature T derived from the kinetic equations for multi-component reacting flows [1]. For 1-D steady-state inviscid flow in the relaxation zone behind the plane shock wave governing equations take the form:

$$\frac{d(vn_{ci})}{dx} = R_{ci}^{vibr} + R_{ci}^{2 \leftrightarrow 2} + R_{ci}^{2 \leftrightarrow 3}, \quad i = 0, 1, \dots, l_c, \quad c = N_2, O_2, \quad (9)$$

$$\frac{d(vn_c)}{dx} = R_c^{2 \leftrightarrow 2} + R_c^{2 \leftrightarrow 3}, \quad c = NO, N, O, \quad (10)$$

$$\rho_0 v_0^2 + p_0 = \rho v^2 + p, \quad (11)$$

$$h_0 + \frac{v_0^2}{2} = h + \frac{v^2}{2}. \quad (12)$$

Here $p = nk_B T$ is the pressure, k_B is the Boltzmann constant, ρ , n are the mass and number mixture densities, index «0» indicates the values of parameters in the free stream, l_c ($c = N_2, O_2$) are the total numbers of excited vibrational levels of N_2 and O_2 molecules, x is the distance from the shock front, h is the enthalpy of the mixture in the unit mass:

$$h = \sum_c h_c Y_c, \quad (13)$$

$$h_c = \frac{5}{2} \bar{R}_c T + \frac{\varepsilon_c}{m_c} \quad \text{for } c = N, O, \quad (14)$$

$$h_c = \frac{7}{2} \bar{R}_c T + \frac{1}{\rho_c} \sum \varepsilon_i^c n_{ci} + \frac{\varepsilon_c}{m_c} \quad \text{for } c = N_2, O_2, NO, \quad (15)$$

where \bar{R}_c is the specific gas constant of species c , m_c is a particle mass, ε_c is the formation energy of a particle c species, $Y_c = \rho_c / \rho$ are the mass fractions of molecules and atoms.

The vibrational energies ε_i^c are simulated using the anharmonic oscillator model with $l_{N_2} = 46$ and $l_{O_2} = 35$ as well as for harmonic oscillators with $l_{N_2} = 32$ and $l_{O_2} = 25$. The source terms in Eqs. (9)-(10) describe vibrational energy transitions (1)-(3) and chemical reactions (4)-(8) and contain state-specific rate coefficients of these processes. The expressions for R_{ci}^{vibr} and $R_{ci}^{2 \leftrightarrow 3}$ are presented in details in [1]. Let us consider the terms $R_{N_2i}^{2 \leftrightarrow 2}$ and $R_{O_2i}^{2 \leftrightarrow 2}$:

$$R_{N_2i}^{2 \leftrightarrow 2} = n_{NO} n_N k_{NO, N_2i}^{N, O} - n_{N_2i} n_O k_{N_2i, NO}^{O, N}, \quad (16)$$

$$R_{O_2i}^{2 \leftrightarrow 2} = n_{NO} n_O k_{NO, O_2i}^{O, N} - n_{O_2i} n_N k_{O_2i, NO}^{N, O}, \quad (17)$$

here $k_{N_2i, NO}^{O, N}$, $k_{O_2i, NO}^{N, O}$ and $k_{NO, N_2i}^{N, O}$, $k_{NO, O_2i}^{O, N}$ are the state-dependent rate coefficients of forward and backward reactions (4)-(5).

Theoretical and experimental data on rate coefficients for vibrational energy transitions and chemical reactions are widely presented in the literature (see, for example [8]). In this paper for VV , VV' and VT transitions, we used generalized formulae [12, 8] of the classical Schwartz, Slawsky and Herzfeld theory. Dissociation rate coefficients are calculated using the Treanor-Marrone model [13] modified for the state-to-state approach in [1].

State-dependent rate coefficients for the forward exchange reactions (4) and (5) are obtained with the use of the analytical expressions proposed in [9]:

$$k_{fci}(T) = C(i+1)T^\beta \exp\left(-\frac{E_a - \varepsilon_i^c}{k_B T} \tilde{\Theta}(E_a - \varepsilon_i^c)\right), \quad (18)$$

where E_a is the activation energy, $\tilde{\Theta}$ is the Heaviside function, $C = 4.17 \times 10^{12}$, $\beta = 0$ for reaction (4), and $C = 1.15 \times 10^9$, $\beta = 1$ for reaction (5), the rate coefficients k_{fci} are in $\text{cm}^3(\text{mol} \cdot \text{s})^{-1}$. Rate coefficients of recombination and backward exchange reactions are found using the detailed balance principle [1].

THREE-TEMPERATURE AND ONE-TEMPERATURE APPROACHES

The analysis of the data on probabilities of vibrational energy transitions shows that the most probable collisions are those resulting in the near resonant VV vibrational energy exchange (1) [8, 12]. In such a collision, two colliding molecules exchange vibrational quanta. Taking into account the conservation of the number of quanta during VV collisions, the non-equilibrium quasi-stationary solution of master equations for an isolated one-component system of anharmonic oscillators was obtained in [14] and later derived from the kinetic equations for the flows of reacting multi-component mixtures [6]. For level populations of the considered air components we have:

$$n_{ci}^T = \frac{n_c}{Z_c^{\text{vibr}}(T, T_1^c)} \exp\left(-\frac{\varepsilon_i^c - i\varepsilon_1^c}{k_B T} - \frac{i\varepsilon_1^c}{k_B T_1^c}\right). \quad (19)$$

Here T_1^c are the vibrational temperatures of the first level for species $c = \text{N}_2, \text{O}_2$, $Z_c^{\text{vibr}}(T, T_1^c)$ are the non-equilibrium partition functions:

$$Z_c^{\text{vibr}}(T, T_1^c) = \sum_{i=0}^{l_c} \exp\left(-\frac{\varepsilon_i^c - i\varepsilon_1^c}{k_B T} - \frac{i\varepsilon_1^c}{k_B T_1^c}\right).$$

For harmonic oscillators the expressions (19) are reduced to the non-equilibrium Boltzmann distributions with vibrational temperatures $T_v^c = T_1^c$.

On the basis of the distributions (19), the equations (9) for vibrational level populations of N_2 and O_2 molecules are reduced to two equations for number densities n_{N_2} and n_{O_2} and two equations for temperatures $T_1^{\text{N}_2}$, $T_1^{\text{O}_2}$. The closed description of the flow in this case is given by 9 equations for number densities of species, gas velocity and three temperatures instead of 88 equations (9)-(12) in the state-to-state approximation. The temperatures T_1^c are connected with the total numbers W_c of vibrational quanta of species c per unit mass:

$$\rho_c W_c(T, T_1^c) = \sum_{i=0}^{l_c} i n_{ci}^T(T, T_1^c), \quad c = \text{N}_2, \text{O}_2. \quad (20)$$

Governing equations in the three-temperature approach include the equations of non-equilibrium vibrational-chemical kinetics [6]:

$$\frac{d(vn_c)}{dx} = R_c^{2 \leftrightarrow 2} + R_c^{2 \leftrightarrow 3}, \quad c = \text{N}_2, \text{O}_2, \text{NO}, \text{N}, \text{O}, \quad (21)$$

$$\rho_c \frac{d(vW_c)}{dx} = R_c^w - m_c W_c (R_c^{2 \leftrightarrow 2} + R_c^{2 \leftrightarrow 3}), \quad c = \text{N}_2, \text{O}_2, \quad (22)$$

$$R_c^w = \sum_{i=0}^{l_c} i R_{ci}^{\text{vibr}}, \quad R_c^{2 \leftrightarrow 2} = \sum_i R_{ci}^{2 \leftrightarrow 2}, \quad R_c^{2 \leftrightarrow 3} = \sum_i R_{ci}^{2 \leftrightarrow 3},$$

and conservation equations in the form (11)-(12). In Eqs. (13)-(15) the total mixture enthalpy and vibrational energy are defined by the distributions (19) and therefore depend on three temperatures T , $T_1^{\text{N}_2}$, $T_1^{\text{O}_2}$ and number densities of species.

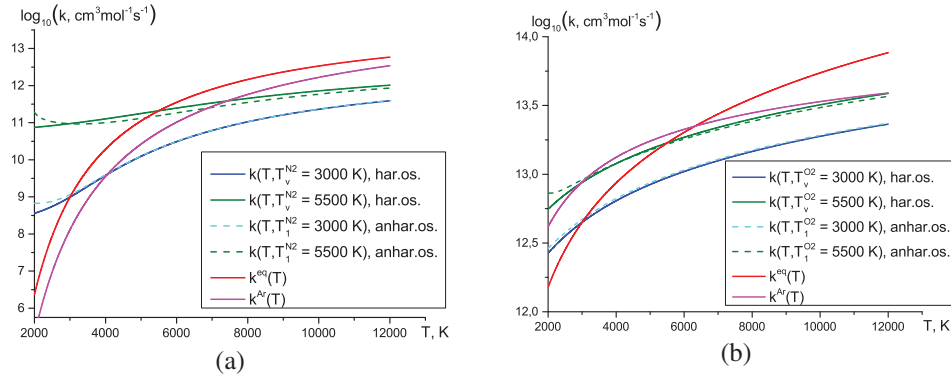


FIGURE 1. The rate coefficients k_{fc} of reaction (4) (a) and reaction (5) (b) as functions of the gas temperature.

The relaxation terms $R_c^{2 \leftrightarrow 2}$, $R_c^{2 \leftrightarrow 3}$ in Eqs. (21) and (22) contain two-temperature rate coefficients for exchange reactions and dissociation which may be found in result of averaging of state-specific rate coefficients over vibrational levels of reacting N_2 and O_2 molecules with the distributions (19).

For rate coefficients of dissociation we use the expressions given in [1]:

$$k_{c,diss}^M = Z_c^M(T, T_1^c, U_c) k_{c,diss-eq}^M(T), \quad c = N_2, O_2, \quad (23)$$

where Z_c^M is the two-temperature non-equilibrium factor:

$$Z_c^M(T, T_1^c, U_c) = \frac{Z_c^{vibr}(T)}{Z_c^{vibr}(-U_c) Z_c^{vibr}(T, T_1^c)} \sum_i \exp \left[\frac{i \varepsilon_i^c}{k_B} \left(\frac{1}{T} - \frac{1}{T_1^c} \right) + \frac{\varepsilon_i^c}{k_B U_c} \right],$$

here $U_c = D_c/6k_B$, D_c is the dissociation energy, $Z_c^{vibr}(T)$ and $Z_c^{vibr}(-U_c)$ are the equilibrium vibrational partition functions, $k_{c,diss-eq}^M$ is the thermal equilibrium dissociation rate coefficient calculated using the Arrhenius formula.

The coefficients of forward exchange reactions (4)-(5) are presented in the form:

$$k_{fc}(T, T_1^c) = \frac{1}{n_c} \sum_i n_{ci} k_{fci}(T), \quad c = N_2, O_2, \quad (24)$$

where state-specific coefficients $k_{fci}(T)$ are found with the use of Eq. (18).

Figures. 1a and 1b present the two-temperature rate coefficients $k_{fc}(T, T_1^c)$ of forward reactions (4) and (5) in dependence on T for different values T_1^c . Rate coefficients increase with T and T_1^c rising, we can notice slight influence of anharmonicity on the coefficients values. The coefficients $k_{fc}(T, T_1^c)$ for reaction (5) are found higher than those for reaction (4). The same figures depict the one-temperature rate coefficients calculated by averaging state-specific coefficients (18) over the equilibrium Boltzmann distributions (k_{fc}^{eq}) and using the Arrhenius expression (k_{fc}^{Ar}). Closer agreement between these values is found for the reaction (5). The coefficients $k_{fc}(T, T_1^c)$ occur less than $k_{fc}^{eq}(T)$ if $T > T_1^c$ and higher than $k_{fc}^{eq}(T)$ for $T < T_1^c$.

Rapid VV' and VT transitions result in equalizing of vibrational temperatures to the gas temperature $T_1^{N_2} = T_1^{O_2} = T$ and establishment of the thermal equilibrium Boltzmann distributions with the gas temperature. In this case the equations for macroscopic parameters n_{N_2} , n_{O_2} , n_{NO} , n_N , n_O , v , T include the equations for non-equilibrium chemical kinetics in the form similar to (21) with the one-temperature reaction rate coefficients and conservation equations (11)-(12). The vibrational energy is defined by the thermal equilibrium distributions and depends only on mixture composition and the gas temperature.

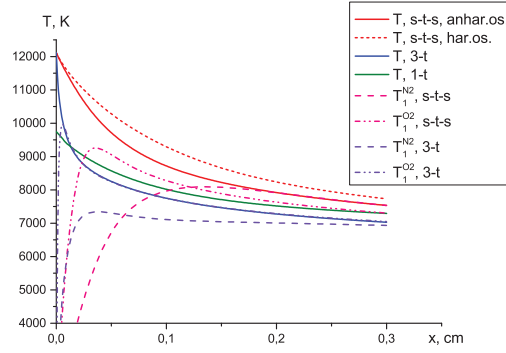


FIGURE 2. The temperatures T , $T_1^{N_2}$, and $T_1^{O_2}$ as functions of x .

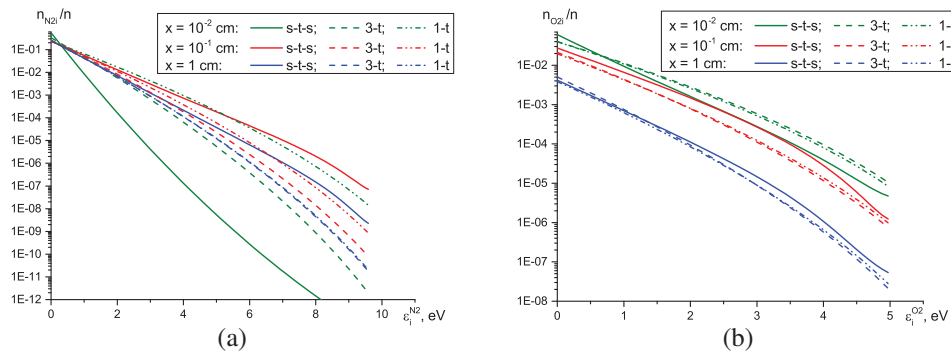


FIGURE 3. The vibrational level populations molecules N_2 (a) and O_2 (b). The curves correspond to different values of x .

RESULTS

In this section we present the flow parameters and vibrational distributions obtained in the relaxation zone behind the shock wave under the following conditions in the free stream: $p_0 = 100$ Pa, $T_0 = 271$ K, $n_{N_2} = 0.79n$, $n_{O_2} = 0.21n$ ($n = p_0/k_B T_0$), $n_{NO} = n_N = n_O = 0$, $M_0 = 15$. These conditions correspond to the altitudes about 48 km and free stream velocities about 5.15 km/sec. The vibrational distributions in the free stream are assumed to be equilibrium with the gas temperature $T_1^{N_2} = T_1^{O_2} = T_0$. The non-equilibrium free stream conditions are considered in [15]. In the state-to-state and three-temperature approaches the gas flow parameters just behind the shock front have been found from the Rankin-Hugoniot relations with the constant mixture composition and vibrational temperatures. In the one-temperature approach the vibrational distributions at $x = 0$ have been supposed to be thermal equilibrium with the gas temperature just behind a shock.

The gas temperature obtained in three considered approaches and vibrational temperatures are presented in Fig. 2. The vibrational temperatures T_1^c ($c = N_2, O_2$) along the relaxation zone have been found in the three-temperature approach and also using the expression following from Eq. (19) for $i = 1$ and connecting T_1^c with populations of the first level n_{c1} [12] in the state-to-state approach. We can notice two effects. First, simplified three-temperature and one-temperature approaches provide underestimated temperature values compared to the state-to-state description. The reason is that these models assume the existence of quasi-stationary distributions just behind a shock and do not describe correctly the process of vibrational excitation close to the shock front. Therefore in the three-temperature approach the process of an increase of vibrational temperatures due to TV activation and decrease due to chemical reactions proceeds much faster than within the state-to-state description. Second, neglecting anharmonicity of vibrations we obtain higher values of T (up to 7%) than for anharmonic oscillators.

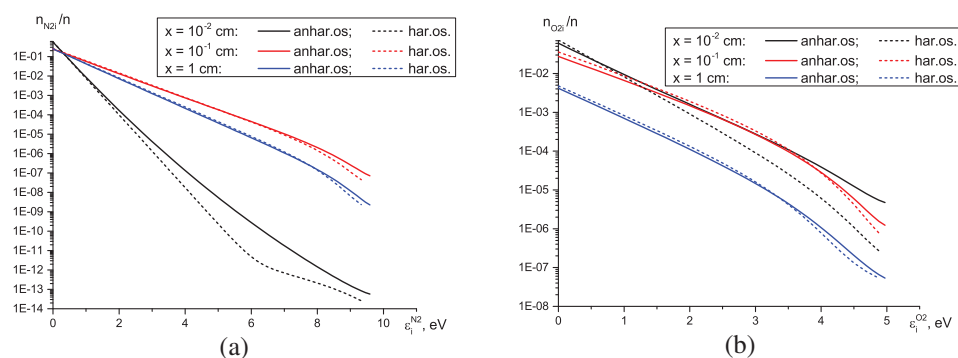


FIGURE 4. The vibrational level populations molecules N_2 (a) and O_2 (b). The curves correspond to different values of x .

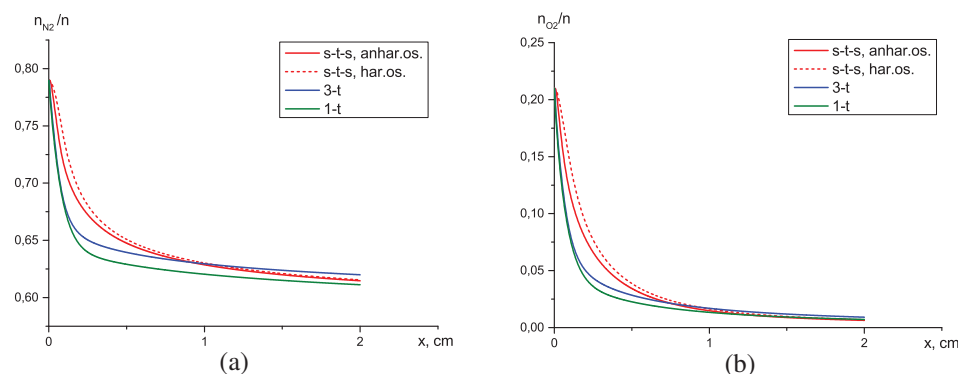


FIGURE 5. The molecular molar fractions n_{N_2}/n (a) and n_{O_2}/n (b) behind the shock front as functions of x .

It is interesting to look at vibrational level populations of N_2 and O_2 molecules found also in three approaches presented in Figs. 3a and 3b versus vibrational energies for three x values. Figure. 3a shows a considerable difference between the vibrational level populations calculated in different approaches close to the shock front, where the quasi-stationary distributions have not been established yet. It is seen that within the state-to-state model nitrogen molecules pass through a stage of excitation and then deactivate whereas the three-temperature model shows very narrow an activation zone (it is 18 and 5 free path lengths in the state-to-state and three-temperature approaches, respectively). In the one-temperature mixture the activation zone is absent completely. That is why the simplified approaches overestimate the level populations in the beginning of the relaxation zone. Activation of oxygen molecules (Fig. 3b) proceeds much faster and then their active participation in chemical reactions leads to rapid decrease of level populations.

Figures. 4a and 4b present the vibrational distributions of N_2 and O_2 molecules for different distances from the shock found for anharmonic and harmonic oscillators. Ignoring anharmonicity leads to the underpopulated levels with higher vibrational energies and weakly overpopulated levels with lower energies as a consequence of slower vibrational energy transitions. The difference in level populations found for anharmonic and harmonic oscillators does not exceed an order of magnitude and decreases with x rising.

Evolution of the mixture composition along the relaxation zone is demonstrated in Figs. 5-7. In Figs. 5a and 5b we compare the number densities of nitrogen and oxygen molecules calculated in three approaches. We can notice that both simplified models underestimate the number densities of N_2 and O_2 molecules. The maximum difference from the values obtained within the state-to-state approach reaches 34% for the one-temperature model and 22% for the three-temperature approach.

On the contrary, reduced models overestimate atomic number densities (Figs. 6) up to 72% for the one-temperature model and 70% for the three-temperature model close to the shock. It is seen that the one-temperature model does not describe the delay of dissociation and exchange reactions close to the shock which is found more evident in the

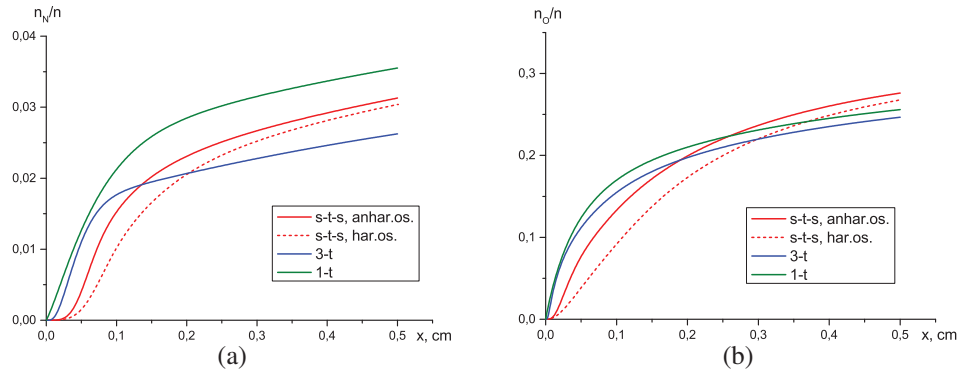


FIGURE 6. The atomic molar fractions n_N/n (a) and n_O/n (b) behind the shock front as functions of x .

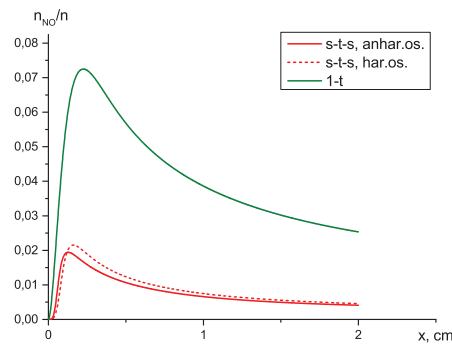


FIGURE 7. The molar fraction n_{NO}/n behind the shock front as functions of x .

state-to-state model and is known from experimental results.

Figure. 7 shows non-monotonous variation of NO molar fractions with x rising: first, an increase due to forward reactions (4) and (5), then decrease in result of the backward reactions. The low values of n_{NO} and n_N are explained by weak N_2 dissociation, active reaction (4) in the reverse direction and forward reaction (5). Similarly to atomic number densities, the one-temperature model greatly overestimates NO number densities.

The harmonic oscillator model provides overestimated N_2 and O_2 number densities, underestimated atom number densities and slows down formation and decomposition of NO molecules.

Results show that the discrepancy between the values found within different models reduces with the distance from the shock front and the mixture approaching to the thermal and chemical equilibrium.

CONCLUSIONS

The non-equilibrium vibrational and chemical kinetics in shock heated air flows is studied on the basis of the state-to-state and simplified approaches and the accuracy of reduced models is estimated.

The influence of a kinetic model on flow parameters is found very important in the region close to the shock front, particularly for vibrational distributions. Then the difference between the models decreases with the mixture approaching to the thermal equilibrium.

Neglect of anharmonicity leads to higher values of the gas temperature and number densities of N_2 and O_2 molecules, lower densities of atoms and tardy formation and decomposition of NO molecules. The anharmonicity effects in the relaxation zone decrease with x rising.

ACKNOWLEDGMENTS

The research leading to these results has received funding from the Russian Foundation for Basic Research (project 12-08-00826) and Saint Petersburg State University (projects 6.38.73.2012 and 6.37.163.2014). We are grateful to Saint-Petersburg State University for the travel grants 6.41.709.2014 and to the RGD29 Local Organizing Committee for supporting O. Kunova in the frame of the Young Scholar Researcher Support program.

REFERENCES

1. E. Nagnibeda, and E. Kustova, *Nonequilibrium Reacting Gas Flows. Kinetic Theory of Transport and Relaxation Processes*, Springer-Verlag, Berlin, 2009.
2. G. Colonna, M. Tuttafesta, M. Capitelli, D. Giordano, *J. Thermophys. Heat Transfer* **13**, 372–375 (1999).
3. S. Bazilevich, K. Sinitsyn, E. Nagnibeda, “Non-Equilibrium Flows of Reacting Air Components in Nozzles,” in *26th International Symposium on Rarefied Gas Dynamics*, edited by T. Abe, AIP Conference Proceedings 1084, American Institute of Physics, New York, 2008, pp. 843–848.
4. M. Capitelli, I. Armenise, C. Gorse, *J. Thermophys. Heat Transfer* **11**, 570–578 (1997).
5. C. Park, *J. Thermophys. Heat Transfer* **20**, 689–698 (2006).
6. A. Chikhaoui, J. Dudon, S. Genieys, E. Kustova, E. Nagnibeda, *Phys. Fluids* **12**, 220–232 (2000).
7. G. Colonna, I. Armenise, D. Bruno, M. Capitelli, *J. Thermophys. Heat Transfer* **20**, 477–486 (2006).
8. G. Chernyi, S. Losev, S. Macheret, B. Potapkin, *Physical and Chemical Processes in Gas Dynamics*, American Institute of Aeronautics and Astronautics, USA, 2004.
9. J. Warnatz, U. Riedel, R. Schmidt, “Different levels of air dissociation chemistry and its coupling with flow models,” in *Advanced in Hypersonic Flows*, edited by J. J. Bertin et al., Birkhäuser, Boston, 1992, pp. 67–103.
10. D. Bose, G.V. Candler, *J. Chem. Phys.* **104**, 2825–2833 (1996).
11. D. Bose, G.V. Candler, *J. Chem. Phys.* **107**, 6136–6145 (1997).
12. B. Gordiets, A. Osipov, L. Shelepin, *Kinetic Processes in Gases and Molecular Lasers*, Gordon and Breach Science Publishers, Amsterdam, 1988.
13. P. Marrone, C. Treanor, *Phys. Fluids* **6**, 1215–1221 (1963).
14. C. Treanor, I. Rich, R. Rehm, *J. Chem. Phys.* **48**, 1798–1807 (1968).
15. O. Kunova, E. Kustova, M. Mekhonoshina, E. Nagnibeda, “The influence of state-to-state kinetics on diffusion and heat transfer behind shock waves,” in *Abstract book of 29th International Symposium on Rarefied Gas Dynamics*, edited by J. Fan, 2014, p. 287.